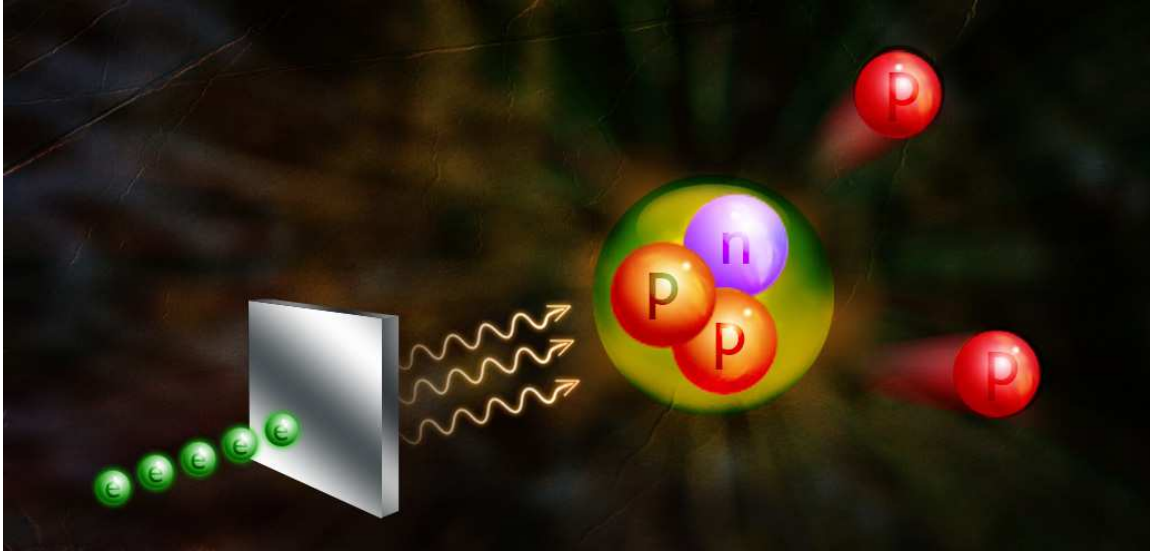


# Hard photodisintegration of ${}^3\text{He}$ into p-p, p-n, and p-d pairs

*The Jefferson Lab Hall A Collaboration*



W. Boeglin, P. Markowitz

*Florida International University, Miami, FL 33199 USA*

G. Ron

*Hebrew University of Jerusalem, Jerusalem, Israel*

D.W. Higinbotham (spokesperson), B. Sawatzky, S. Wood

*Jefferson Lab, Newport News, VA 23606 USA*

W. Bertozzi, S. Gilad

*Massachusetts Institute of Technology, Cambridge, MA 02139 USA*

L. Weinstein

*Old Dominion University, Norfolk, VA 23529 USA*

L. El Fassi, R. Gilman (spokesperson), S. Leighton

G. Kumbartzki, R. Ransome, Y. Zhang

*Rutgers University, Piscataway, NJ 08854-8019 USA*

D. Anez, A.J. Sarty

*St. Mary's University, Halifax, Nova Scotia B3H 3C3 CANADA*

N. Bubis, O. Hen, I. Korover, E. Piasetzky,

I. Pomerantz (spokesperson and contact person), R. Shneur

*Tel Aviv University, Tel Aviv, Israel*

S. Širca, M. Mihovilović

*University of Ljubljana, Jadranska 19, 1000 Ljubljana, SLOVENIA*

S. Strauch (spokesperson), Y. Ilieva

*University of South Carolina, Columbia, South Carolina 29208, USA*

G. Jin, R. Lindgren, B.E. Norum

*University of Virginia, Charlottesville, Virginia 22904, USA*

## ABSTRACT

Extensive studies of high-energy deuteron photodisintegration over the past two decades have probed the limits of meson-baryon descriptions of nuclei and reactions. At high energies, photodisintegration cross sections have been shown to follow the constituent counting rules, which suggests that quarks are the relevant degrees of freedom.

In an attempt to more clearly identify the underlying dynamics at play in high-energy nuclear photodisintegration, E03-101 measured, in 2007, the hard photodisintegration of two protons, using  $^3\text{He}$ . The basic idea is that theoretical models should be able to predict the relative size of pp versus pn disintegrations. The results from E03-101 clearly indicate the onset of scaling; but due to the cross section being smaller than expected, the statistics were insufficient to determine the underlying mechanism that produces high transverse momentum proton pairs. Preliminary data on a two body hard breakup of  $^3\text{He}$  to p-d pairs are also available from that experiment over a small  $s$ -range.

We propose here a second generation measurement of hard photodisintegration of  $^3\text{He}$  into np, pp, and pd pairs. The experiment is aimed at addressing issues the previous measurements and current theory are insufficient to resolve:

1. A measurement of both  $\gamma\ ^3\text{He} \rightarrow \text{pp}(n)$  and  $\gamma\ ^3\text{He} \rightarrow \text{pn}(p)$  will address the issue of the small ratio of  $\gamma\ ^3\text{He} \rightarrow \text{pp}(n)$  to  $\gamma\ d \rightarrow \text{pn}$ .
2. High quality data over a large  $s$ -range on the two body break-up of  $\gamma\ ^3\text{He} \rightarrow \text{pd}$  will confirm the scaling of the invariant cross section as a function of  $s$  and determine the power with a small uncertainty.
3. Higher statistics for  $\gamma\ ^3\text{He} \rightarrow \text{pp}(n)$  will provide a conclusive check to determine if hard re-scattering is the correct dynamical treatment to explain the production of high  $P_T$  nucleons as proposed.

The experimental hall beam time request is for 19 days. No new equipment and no special setup or development time are required. This measurement does not need the 12 GeV upgrade but JLab is the only facility world wide at which such a measurement can be done.

# 1 Scientific background and motivation

## 1.1 Overview

There is a strong theoretical bias that at high enough energy exclusive reaction cross sections should scale according to the constituent counting rule (CCR),

$$\frac{d\sigma}{dt} \propto s^{2-n_i-n_f} \quad (1)$$

at constant center-of-mass (c.m) angle, where  $n_i$  ( $n_f$ ) is the total number of point-like particles in the initial (final) state – e.g.,  $n = 3$  for a nucleon. The CCR was originally derived from dimensional analysis [1, 2], rederived from perturbative quantum chromodynamics (pQCD) [3], extended to include the effects of orbital angular momentum [4], and rederived again from the AdS/CFT correspondence of string theory [5]. Since the CCR is based on the number of quarks in a hadronic reaction, one expects that kinematic variables such as Mandelstam  $s$  (total energy in c.m. squared),  $t$  (four-momentum transferred from beam to outgoing particle), and  $u$  (four-momentum transfer from beam to residual) must all be large compared to the QCD scale,  $\Lambda_{QCD}$ , but there is no theoretical guidance as to exactly how large they must be. Nevertheless, many reaction cross sections are found to scale starting at GeV energies, even though the best pQCD calculations to date severely underestimate the magnitude of the cross sections. It remains a mystery why this is so, and why various reactions do or do not scale.

A number of high-energy exclusive hadronic and nuclear reactions have been measured to date. Meson photoproduction from the nucleon and meson-baryon scattering are generally consistent with scaling for energies above the resonance region. Real Compton scattering however is inconsistent with scaling, falling as  $s^{-8}$  rather than  $s^{-6}$  [6]. The energy dependence is reminiscent of meson-baryon scattering, which suggests an explanation in terms of the hadronic component of the photon is possible [7], but the cross sections have also been successfully calculated using the handbag diagram [8].

Nucleon-nucleon elastic scattering has long been known to have oscillations about the expected  $s^{-10}$  scaling as well as an interesting spin structure [9]. The behavior has been attributed to charm thresholds [10], or alternatively to the interference of quark-exchange and Landshoff (multi-gluon exchange) mechanisms [11, 12].

With one exception, high-energy nuclear studies to date have used only the deuteron, the lightest, and only  $A = 2$ , nucleus [13, 14, 15, 16, 17, 18, 19, 20]. The most studied nuclear reaction is deuteron photodisintegration,  $\gamma d \rightarrow pn$ . Scaling is observed at all angles as long as  $p_T$ , the transverse momentum of the outgoing nucleons,  $\gtrsim 1.3$  GeV/ $c$ . This corresponds to a photon energy just over 1 GeV for  $\theta_{c.m.} = 90^\circ$ , and higher at other angles. The scaling at  $90^\circ$  is good to perhaps 10% while the cross section drops a factor of 30,000 as the beam energy increases from 1 to 4 GeV.

Recently, two-proton disintegration has been observed on a  $^3\text{He}$  target, with a neutron spectator [21]. Scaling is observed to start at  $\sim 2$  GeV photon energy, with scaled cross sections a factor of  $20^1$  smaller than in the deuteron  $pn$  case. Below 2 GeV there is a peak in the cross section, multiplied by  $s^{11}$ , which might indicate underlying dynamics of resonance excitation.

We also recently extended the search for scaling in the  $A=3$  system to the  $\gamma^3\text{He} \rightarrow pd$  reaction. As previous measurements have only involved  $A = 1$  or  $2$ , the expected scaling degree of  $d\sigma/dt \propto s^{-17}$  is higher power than any previously observed.

---

<sup>1</sup>  $\frac{d\sigma}{dt}[d(\gamma,p)n]}{\frac{d\sigma}{dt}[^3\text{He}(\gamma,pp)n]} \sim 40$ , an additional factor of 0.5 accounts for the relative abundance of p-p pairs having cm momentum up to 100 MeV/ $c$ .

The measurement proposed here aims to address open CCR issues raised by the available data.

1. We propose to compare directly  $\gamma \text{ }^3\text{He} \rightarrow \text{pp}$  to  $\gamma \text{ }^3\text{He} \rightarrow \text{pn}$  to verify the insight as to the reason for the large unexplained ratio of  $\gamma \text{ }^3\text{He} \rightarrow \text{pp}$  to  $\gamma \text{ d} \rightarrow \text{pn}$  cross section ratio, without the theoretical arguments needed to compare production of two nucleons from the deuteron with two nucleons from  $\text{ }^3\text{He}$ .
2. We propose to gather high quality data on the two body break-up of  $\gamma \text{ }^3\text{He} \rightarrow \text{pd}$  over a large  $s$  range. High precision confirmation of the invariant cross section  $s^{-17}$  scaling, as suggested by the previous data, can validate the CCR prediction for the  $A>3$  system.
3. We propose to make a conclusive check to determine if Hard Re-scattering is the correct dynamics to explain the production of high  $p_T$  nucleons in the hard photodisintegration process.

## 1.2 Hard photodisintegration of $\text{ }^3\text{He}$

We define a hard photodisintegration as a process in which a high energy photon is absorbed by a nucleon system and as a result the system disintegrates into two sub-systems, which are emitted with large transverse momenta, greater than about 1 GeV/c. As defined in this process, the Mandelstam parameters  $s$  and  $t$  are large. Below we present the state of the art and the proposed measurement of 3 hard photodisintegration processes with two high momentum particles detected in the final state.

### 1.2.1 $\text{ }^3\text{He}(\gamma, \text{pp})\text{n}$

Figure 1 shows the  $\gamma + \text{d} \rightarrow p + n$  and  $\gamma + \text{ }^3\text{He} \rightarrow p + p + n$  cross section at  $\theta_{c.m.} = 90^\circ$  scaled by  $s^{11}$ . The  $\text{ }^3\text{He}(\gamma, \text{pp})\text{n}$  events were selected with  $p_n < 100$  MeV/c, where  $p_n$  is the neutron momentum. The cross section is compared to predictions for the photodisintegration of both  $\text{pn}$  and  $\text{pp}$  pairs from theoretical models, which are discussed below [22]. In the *scaling* region the cross section for both  $\text{pn}$  and  $\text{pp}$  breakup scales in agreement with the constituent counting rule [1, 3, 5]. For proton-pair break-up, the onset of the scaling is at  $E_\gamma \approx 2.2$  GeV, while for  $\text{pn}$  pairs scaling commences at  $E_\gamma \approx 1$  GeV [18]. The scaling in the  $\text{ }^3\text{He}$  case indicates that in this regime the two-body process is dominant. It further suggests (in a relatively model-independent way) that the relevant degrees of freedom that govern the dynamics are the quarks.

The reduced nuclear amplitude (RNA) formalism [24] after normalization to the deuteron data [22] yields cross sections that are about 200 times larger than the present data. The quark-gluon string model (QGS) [25, 26], as estimated in [22], predicts cross sections about a factor of 5 larger than measured. The QCD hard re-scattering model (HRM) [27] provides an absolute calculation of the cross sections for both  $\text{pn}$  and  $\text{pp}$  pair photodisintegration from nucleon-nucleon measured cross sections without adjustable parameters. It reproduces the deuteron data reasonably well and the proton pair cross section. The HRM model predicts an energy dependence of the scaled cross section that the E03-101 data is not accurate enough to either confirm or reject. We propose here a conclusive check of the HRM prediction.

### 1.2.2 $\text{ }^3\text{He}(\gamma, \text{pd})$

Recently data for two body break-up of  $\text{ }^3\text{He}$  into a proton and a deuteron were collected by two experiments at JLab; Experiment 03-101, which ran in Hall A [28], and Experiment

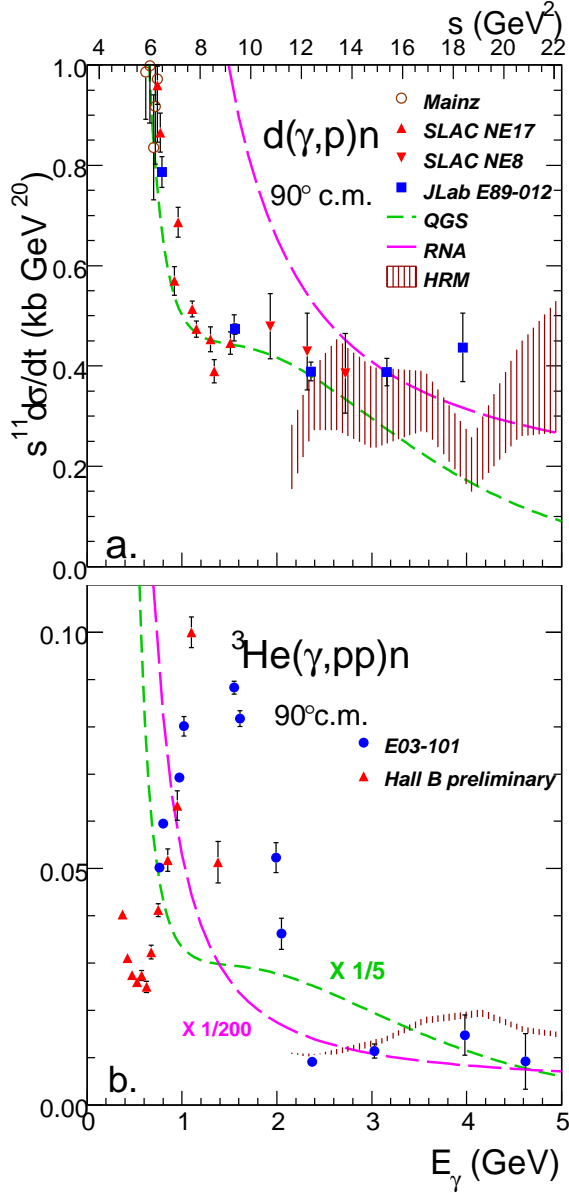


Figure 1: The  $d(\gamma,p)n$  (a) and  ${}^3\text{He}(\gamma,pp)n$  (b) invariant cross section scaled by  $s^{11}$ .  ${}^3\text{He}(\gamma,pp)n$  events were selected with  $p_n < 100$  MeV/c. Up to 2.1 GeV, the photon energy bins are 70 MeV, and above it 140 MeV. Model predictions are taken from [22, 23]. In (b), RNA is divided by a factor of 200 and QGS by a factor of 5 to be shown on this scale. Error bars represent statistical uncertainty. Further details may be found in [21]

g3/CLAS which ran in Hall B [29].

Figure 2 shows the resulting cross sections compared to previously published data [30] for  $s > 10$  GeV<sup>2</sup>. The consistency of the scaled cross sections with being constant can be seen. In the range of the new data,  $E_\gamma = 0.4 - 1.3$  GeV or  $s = 10 - 15$  GeV<sup>2</sup>, the cross section falls by two orders of magnitude. The falloff of our data is fit as  $s^{-18 \pm 1}$ , consistent with the CCR prediction of  $n = 17$ . Work is proceeding on a joint publication of the Hall A and B data. We propose here to extend this measurement over a larger  $s$  range to determine the scaling with better precision.

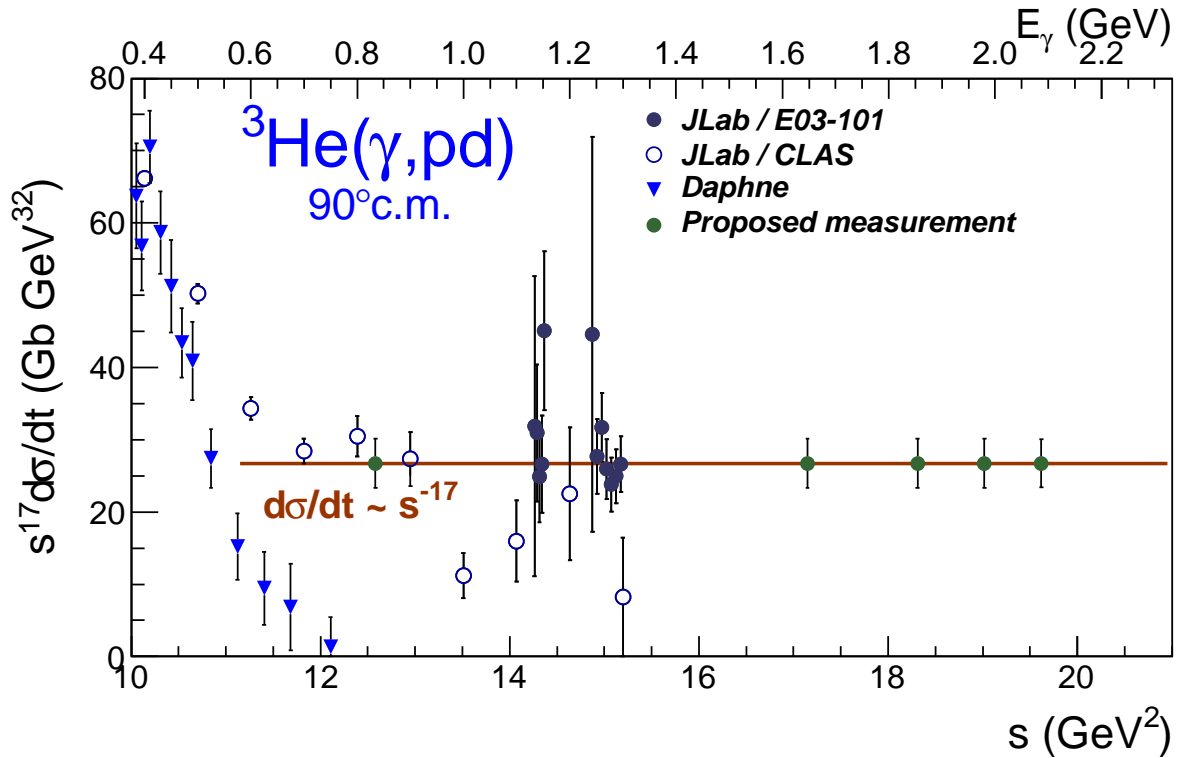


Figure 2: The invariant cross section  $d\sigma/dt$  multiplied by  $s^{17}$  to remove the expected energy dependence. DAPHNE data is taken from [30]. JLab data is taken from [31]. The horizontal line indicates the scaling predicted by the Constituent Counting Rules normalized to the JLab data. The proposed measurement points are shown arbitrarily positioned on the scaling curve with the estimated statistical uncertainty.

### 1.2.3 ${}^3\text{He}(\gamma, \text{pn})\text{p}$

No data exist for hard photodisintegration of a pn pair in  ${}^3\text{He}$ .

## 1.3 The proposed measurements

### 1.3.1 ${}^3\text{He}(\gamma, \text{pp})\text{n}$

**Energy dependence of the cross section** Figure 1 (a.) shows the pp breakup cross section. The uncertainty above 3.1 GeV in the data is dominated by statistics. The four data points (filled circles) are in good agreement with the HRM prediction as well as with scaling (a constant). We propose a measurement to reduce the uncertainty of the  ${}^3\text{He}(\gamma, \text{pp})\text{n}$  cross section in the scaling region, to conclude whether oscillations predicted by the HRM exist. Figure 3 shows the  ${}^3\text{He}(\gamma, \text{pp})\text{n}$  invariant cross sections ratio of 3.0 GeV to 4.4 GeV (photon energy). This ratio can test the HRM prediction for deviation from CCR  $s^{-11}$  scaling. The dominant contribution to the uncertainty is the expected statistics of the high energy measurements. As can be seen in Fig 3, with the expected statistical uncertainty of the proposed measurement, the HRM prediction is different from scaling by 5 standard deviations.

**$\alpha_n$  Distribution** The recoil neutron in  $\gamma {}^3\text{He} \rightarrow \text{pp} + \text{n}$  gives an additional way to check the underlying mechanism of hard pp pair production. The observable which is best suited

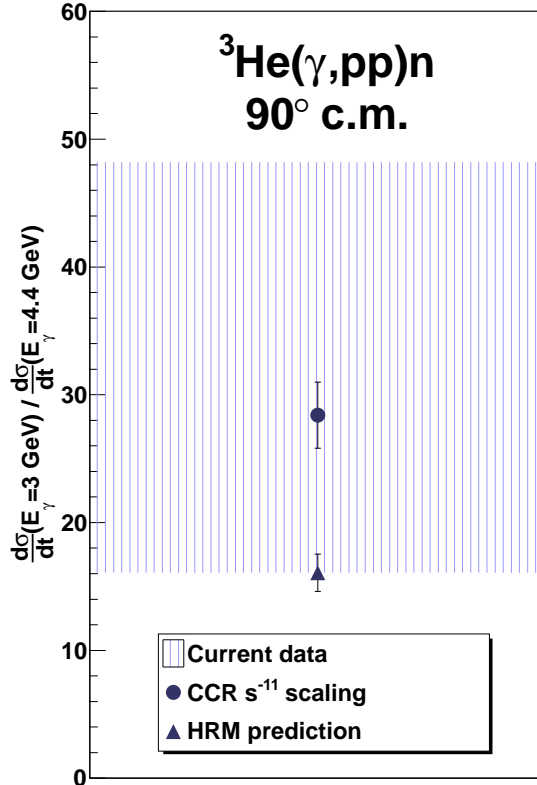


Figure 3: The ratio of the  ${}^3\text{He}(\gamma,pp)n$  invariant cross sections for photon energies of 3.0 GeV to 4.4 GeV. The shaded area indicates the uncertainty from current E03-101 data. The circle indicates Constituents Counting Rules (CCR) prediction of invariant cross section scaling with  $s^{-11}$ . The triangle indicates the HRM prediction. Error bars indicate the statistical uncertainties for the proposed measurement.

for this purpose is the light-cone momentum distribution of the recoil neutron, defined as:

$$\alpha_n = \frac{E_n - p_n^z}{m_{{}^3\text{He}}/3} \quad (2)$$

where the  $z$  direction is chosen in the direction of the incident photon beam.

An important feature of high-energy small-angle final-state rescattering is that it does not significantly change the light-cone fractions of the fast protons – see e.g. [32]. As a result, the experimentally determined  $\alpha_n$  coincides with the value of  $\alpha_n$  in the initial state and measures the light-cone fraction of the two-proton subsystem in the  ${}^3\text{He}$  wave function. Furthermore, in the  ${}^3\text{He}$  wave function the c.m. momentum distribution of the  $NN$  pair depends on the relative momentum of the nucleons in the pair, so one can probe indirectly the magnitude of the momentum in the  $pp$  pair involved in the hard disintegration by the measured neutron alpha distribution.

To illustrate the sensitivity of the  $\alpha_n$  distribution to the mechanism of the high- $p_T$  disintegration of a  $pp$  pair, we compare in Fig. 4 the  $\alpha_n$  dependence of the differential cross section  $\frac{d\sigma}{dt d^2 p_T d\alpha_n / \alpha_n}$  calculated in the framework of the RNA and HRM models. The results presented in Fig. 4 provide substantially different predictions for the  $\alpha_n$  distribution. Qualitatively, the much broader distribution of  $\alpha_n$  in the RNA model is due to the selection of large momenta of protons in the  ${}^3\text{He}$  wave function, which leads to a broader distribution

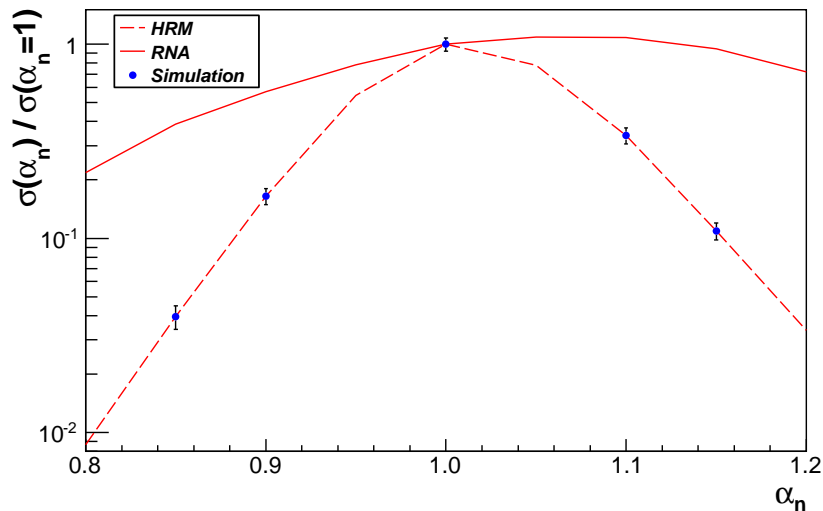


Figure 4:  $\alpha_n$  distribution of the spectator neutron at  $E_e = 2.2$  GeV. Cross section calculated within RNA (bold red solid line) and HRM (bold red dashed line) models, and simulated data points (blue).  $\sigma(\alpha_n)$  corresponds to the differential cross section scaled by  $s_{pp}^{11}$ . Anticipated uncertainties are for the proposed beam-time.

of neutron momenta. The simulated data points were generated by sampling the wave function of the neutron in  ${}^3\text{He}$  [33] up to 100 MeV/ $c$  (same assumption as in the HRM).

### 1.3.2 ${}^3\text{He}(\gamma, \text{pd})$

**Energy dependence of the cross section** We propose to extend the data for high energy  $\gamma$   ${}^3\text{He} \rightarrow \text{pd}$  up to  $s \sim 20$  GeV. The proposed data points (Fig. 2) will complement previous data from Halls A and B [31] and will indicate whether CCR scaling is observed in an  $A > 2$  system at these energies.

### 1.3.3 ${}^3\text{He}(\gamma, \text{pn})\text{p}$

**Angular distribution of the cross section** In an attempt to find the reason for the very low magnitude of the cross section ratio:

$$\frac{\frac{d\sigma}{dt} [{}^3\text{He}(\gamma, \text{pp})n]}{\frac{d\sigma}{dt} [d(\gamma, \text{p})n]} \sim 0.025, \quad (3)$$

found in E03-101 [21], we propose to measure the cross section for the break-up of a p-n pair out of  ${}^3\text{He}$  at various c.m. angles with  $E_\gamma = 2.2$  GeV. The proposed data points are plotted in Fig. 5. These measurement will test the various assumptions made by theory about the treatment of p-n pairs with a spectator p in  ${}^3\text{He}$  vs. a free p-n pair (deuteron). These measurements come with almost no additional beam time since they can be taken in parallel with the  ${}^3\text{He}(\gamma, \text{pd})$  measurement using a third detector to detect the emitted neutron. An angular distribution of the  ${}^3\text{He}(\gamma, \text{pp})n$  cross section for the same kinematics will also be taken for reference. The rates for both reactions are very high (see Table 1) and the required statistics will be gathered in short runs.

### 1.3.4 Summary

Fig. 6 presents the c.m. angle vs. the c.m. energy for  ${}^3\text{He}(\gamma, \text{pd})$ ,  ${}^3\text{He}(\gamma, \text{pp})n$  and  ${}^3\text{He}(\gamma, \text{pn})\text{p}$  measurements. Empty markers indicate available data with less than 10%

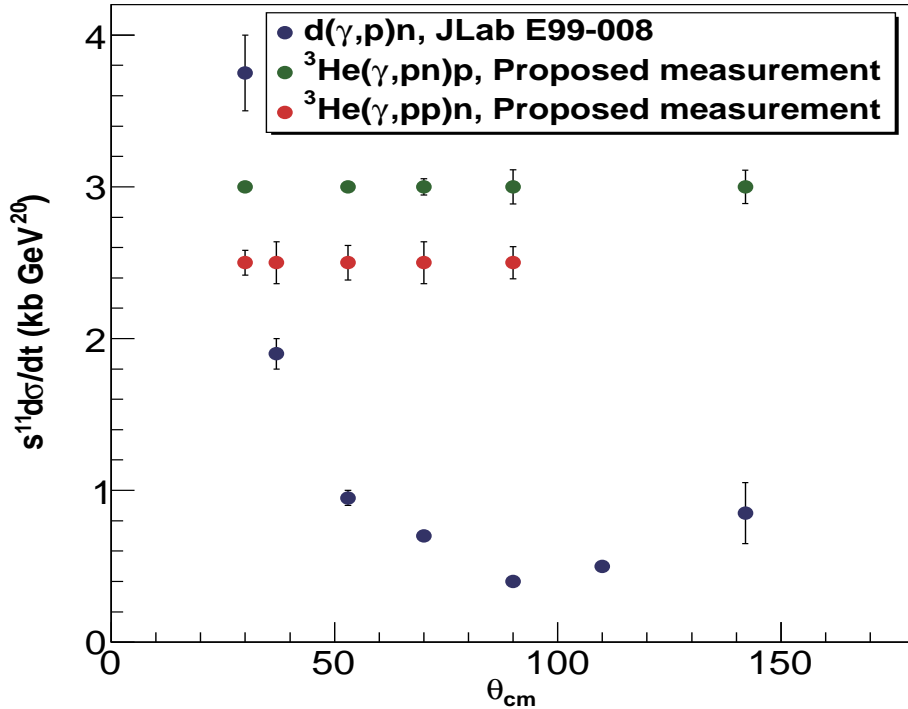


Figure 5: Angular distribution of the invariant cross section scaled with  $s^{11}$  for  $E_\gamma = 2.2$  GeV. Blue points are the available data for  $d(\gamma,p)n$ . The proposed measurements for  ${}^3\text{He}(\gamma,pn)p$  and  ${}^3\text{He}(\gamma,pp)n$  are plotted in green and red respectively.

uncertainty. Full markers indicate the proposed measurements.

## 2 Experimental details

### 2.1 Experimental overview

We propose to measure  $\gamma {}^3\text{He} \rightarrow pp + n_{spec}$ ,  $\gamma {}^3\text{He} \rightarrow pn + p_{spec}$  and  $\gamma {}^3\text{He} \rightarrow pd$  in Hall A. The experimental setup is schematically illustrated in Fig. 7. Bremsstrahlung photons, produced by the electron beam passing through a photon radiator, will impinge on a cryogenic gas  ${}^3\text{He}$  target. The maximum energy of the Bremsstrahlung beam is essentially equal to the incident electron kinetic energy. The target, downstream of the radiator, is irradiated by the photons and the primary electron beam. The experiment will run in two detection modes:

- Detection of two protons in coincidence by the two High Resolution Spectrometers (HRS) (Fig. 7 a.).
- Detection of a proton with one HRS in coincidence with either a deuteron in the other HRS or a neutron in the n-array (Fig. 7 b.).

In the proposed kinematics, each detected particle carries about half the incident beam energy.

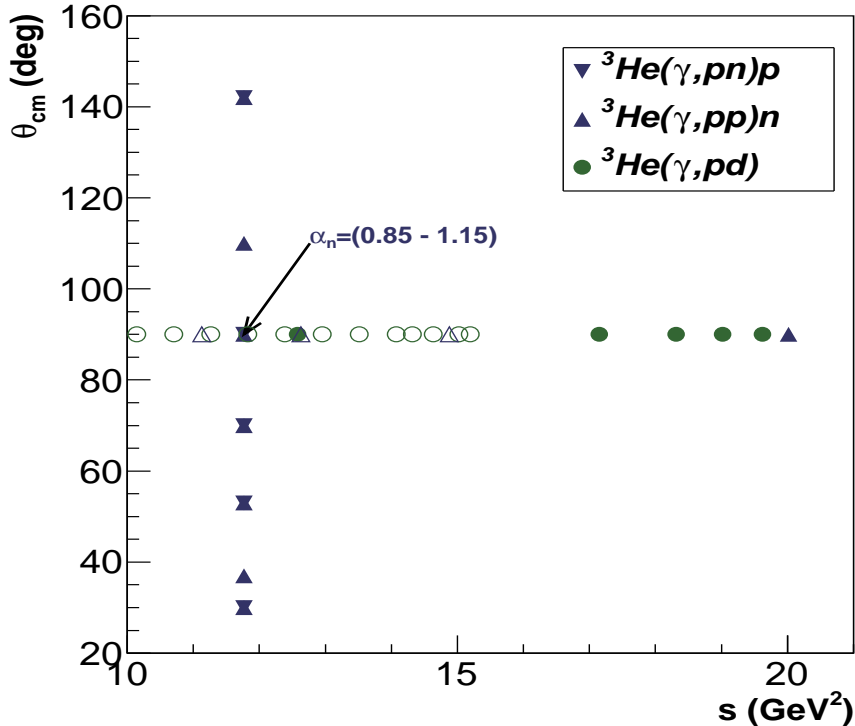


Figure 6: Available data with less than 10% uncertainty (empty markers) and the proposed measurements (full markers) for  ${}^3\text{He}(\gamma, pn)p$ ,  ${}^3\text{He}(\gamma, pp)n$  and  ${}^3\text{He}(\gamma, pd)$ . Note that since the  ${}^3\text{He}(\gamma, pp)n$  is symmetric around 90 degrees c.m., some proposed kinematics are indicated with two points.

## 2.2 Photon radiator

The radiator is the standard Hall A Cu radiator with a 6% radiation length thickness<sup>2</sup>. To limit divergence of the beam and interactions with the target walls and flow diverters, it is preferred to use a radiator foil mounted directly in the cryotarget cell block, about 15 cm upstream of the center of the target. Since the radiator is directly cooled by the cryotarget, melting is not an issue. The main constraint on maximum beam current is the site boundary radiation level. We propose to do the measurement with a 50  $\mu\text{A}$  beam and with the standard cryotarget raster, as has been done in earlier Hall A photodisintegration experiments. The power deposited in the Cu is about 125 W for a beam current of 50  $\mu\text{A}$ .

## 2.3 Target

We will use the 20 cm long narrow “race track” cryotarget cell, which was used in E03-101. That target has proven to be successful both in reducing the uncertainty associated with the cuts (subtractions of end cap background) and decreasing multiple scattering of the ejected particles, which leads to improved momentum and energy resolution. We expect that the target will be able to operate at the same temperature, pressure and density as in the previous run, leading to a  ${}^3\text{He}$  density of 0.079 g/cm<sup>3</sup>.

<sup>2</sup>Although tagged photon beam experiments are generally desirable, the technique is not feasible for high energy, high momentum transfer reactions. The decrease in luminosity makes these small cross sections unmeasurable.

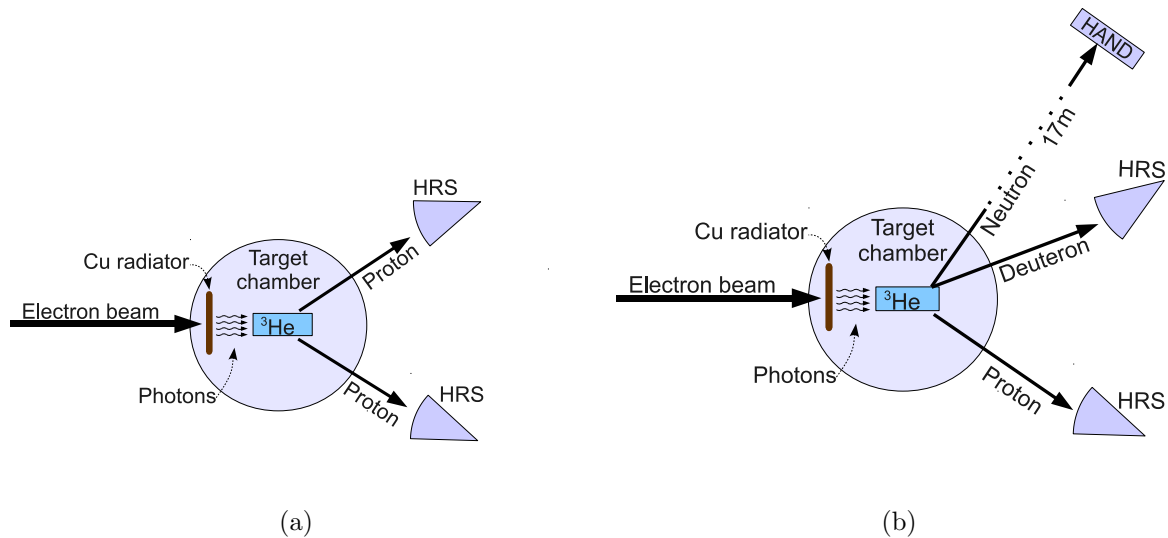


Figure 7: Experimental setup for the measurement of  ${}^3\text{He}(\gamma,pp)n$  (a) and the simultaneous measurement of  ${}^3\text{He}(\gamma,pd)$  and  ${}^3\text{He}(\gamma,pn)p$  (b): Bremsstrahlung photons generated in a copper radiator by an electron beam impinging on a  ${}^3\text{He}$  gas target. Protons and deuterons are detected with the two HRSs. Neutrons are detected with the neutron array. Elements shown are not to scale.

## 2.4 High Resolution Spectrometers (HRS)

We will use the two Hall A spectrometers ( $\text{HRS}_L$  and  $\text{HRS}_R$ ) to measure the two protons in coincidence. This measurement requires no changes from the standard detector package, electronics and operation of the spectrometers. For this experiment, the spectrometer momentum range is  $\approx 1.8 - 3.0$  GeV/c and the angular range is  $42 - 53^\circ$  lab. All necessary equipment including detectors, electronics and data acquisition are already available.

## 2.5 The n-array (HAND)

The Hall A Neutron Detector (HAND) shown in Fig. 8 has been chosen as the neutron detector for two main reasons. First, it is possible to move HAND into and out of position in a short time – HAND is positioned at the same angle for the  $(\gamma, pn)$  measurements as the HRS is for the corresponding  $(\gamma, pp)$  measurements. Second, HAND provides adequate angle and energy resolution for the experiment. HAND was recently reused in experiments E05-102 and E08-005 [34, 35] and will be used again with 2 additional layers in the upcoming E07-006 [36]. HAND is a large volume neutron detector that consists of 112 plastic scintillator bars, divided up into six planes. Each bar is viewed by two photomultiplier tubes, one on each end. The height of the bars in each of the first three planes is 10 cm, 12.5 cm and 15 cm respectively, and 25 cm for the last three planes. The neutron detector also has a veto detector located in front of the first plane. The veto detector consists of 64 plastic bars that are 2 cm thick and are organized into 32 rows of two end-to-end overlapping paddles. HAND needs a crane to setup, and we plan to wire it so placing it in the proposed kinematics does not require rewiring. The kinematic settings have been chosen so there will be no more than one movement of HAND per day, which is expected to take about 4 hours.

For the rates calculation, we simulate HAND as a 3 m (height)  $\times$  1 m (width) detector 17 m from the target. In front of HAND, there will be a lead wall comprised of iron (4 cm thick) and lead (5.1 cm). The distance between the back face of the wall and the front face of HAND is 56 cm.



Figure 8: HAND during the E05-102 run, standing at roughly the proposed angle for this measurement. As can be seen in this picture the cables can be placed so the detector can be easily moved in and out of its place. Not shown in the figure is the lead wall.

Shielding of HAND from neutrons emitted from the radiator will be done by placing a few meters of cement along the line of sight between the radiator and the detector without obstructing the neutrons emitted from the target. The shielding will decrease the singles seen by the n detector by a factor of 2.

## 2.6 Detection acceptance

The finite acceptance correction for the measurement of p-p and p-d pairs in coincidence was determined using the standard Hall A Monte-Carlo simulation software MCEEP [37], and used for the analysis of E03-101 [21, 31].

Another simulation was constructed to evaluate the acceptance and energy resolution for detecting a neutron and a proton in coincidence using the HAND and the HRS respectively. The left panel of Fig 9 shows the angular distribution of the emitted neutron from the  ${}^3\text{He}(\gamma, pn)p$  reaction events in coincidence with a proton detected by the HRS at  $53^\circ$  ( $90^\circ$  in the c.m. of the  $\gamma$ -pn system). The red box indicates the HAND detection acceptance. The number of accepted events for this case compared to the number of accepted  ${}^3\text{He}(\gamma, pp)n$  events (measured by a coincidence between the two HRSs in E03-101), is found to be  $\frac{\text{Accept}\{{}^3\text{He}(\gamma, pn)p\}}{\text{Accept}\{{}^3\text{He}(\gamma, pp)n\}} = 1.46$ .

## 2.7 Reconstructed photon energy

The photon energy for each reaction channel can be calculated event by event from the momentum of the detected particles using momentum/energy conservation. To assure that the kinematic reconstruction is valid, one needs to select only two-body events. This selection is done in two different schemes, both have been previously used in the analysis of E03-101:

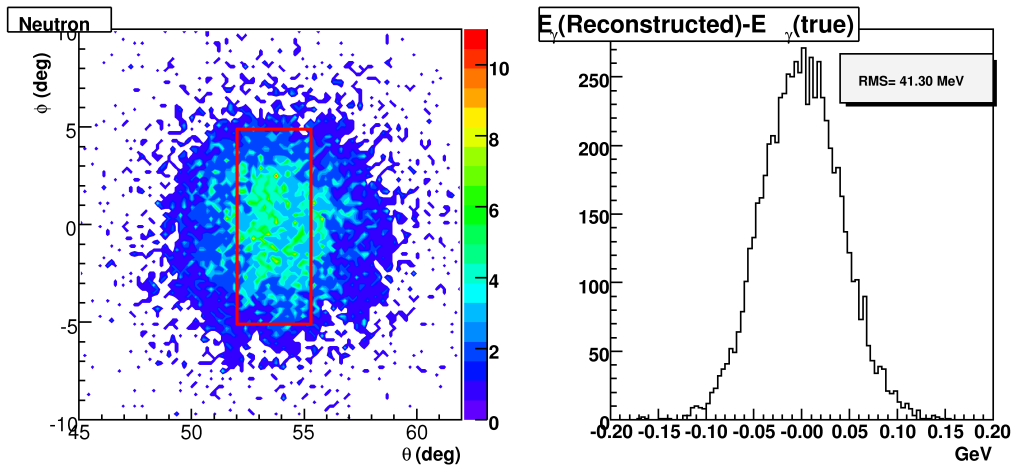


Figure 9:  ${}^3\text{He}(\gamma,\text{pn})\text{p}$  simulation results. On the left panel the angular distribution of the emitted neutron is displayed for events with a proton detected in coincidence by the HRS. The red box indicates the HAND detector acceptance. On the right panel, the simulated resolution of the reconstructed photon energy is shown.

- For  ${}^3\text{He}(\gamma,\text{pp})\text{n}$  and  ${}^3\text{He}(\gamma,\text{pn})\text{p}$  the photon energy is calculated assuming a two-body process. Then, only events which are no more than a 140 MeV (pion production threshold) off the bremsstrahlung tip are selected. This procedure assures that no third particle can be produced.
- For  ${}^3\text{He}(\gamma,\text{pd})$ , the detection of the full final state allows for the selection of events that fulfill two energy and momentum constraints:

1.  $p_{T\text{ missing}} \equiv p_{T(p)} + p_{T(d)} < 5 \text{ MeV}/c$ , and
2.  $\alpha_{\text{missing}} \equiv \alpha_d + \alpha_p - \alpha_{{}^3\text{He}} - \alpha_\gamma < 5 \cdot 10^{-3}$ ,

where the light cone momentum,  $\alpha$ , is defined in Eq. (2). A simulation of pion production for this process shows that with these cuts the contamination of non 2-body events is negligible.

The resolution of the reconstructed photon energy in measuring  ${}^3\text{He}(\gamma,\text{pp})\text{n}$  and  ${}^3\text{He}(\gamma,\text{pd})$  using the two HRSs was studied in the analysis of E03-101 and found to be in the range of a few MeV. For the  ${}^3\text{He}(\gamma,\text{pn})\text{p}$  measurement, the expected photon energy resolution was evaluated in the MC by smearing the known angle and momentum of the detected proton and neutron by the measurement resolution and reconstructing the photon energy with the smeared values. The right panel of Fig 9 shows the expected resolution of the reconstructed photon energy. The resolution is found to be  $\Delta E_\gamma = 41.1 \text{ MeV}$  (r.m.s) which is sufficient to select events which are below the pion production threshold (140 MeV).

## 2.8 Projected rates

The predicted differential cross sections and expected count rates are shown in Table 1. Both the cross sections and count rates have been calculated assuming running conditions of 50  $\mu\text{A}$  current, a 6 % copper radiator and the Hall A unpolarized  ${}^3\text{He}$  target (same conditions as in E03-101). For  ${}^3\text{He}(\gamma,\text{pp})\text{n}$  the cross sections have been calculated based on interpolation from the E03-101 data points. For the  ${}^3\text{He}(\gamma,\text{pd})$  reaction, they were estimated under the assumption of scaling of the invariant cross section with  $s^{-17}$ . For

Table 1: *Estimated cross sections, rates and requested beam time.*

#	$E_e$	Target	Time	$\gamma^3\text{He} \rightarrow \text{pd}$						$\gamma^3\text{He} \rightarrow \text{pn}$						$\gamma^3\text{He} \rightarrow \text{pp}$							
				$E_\gamma$	$s$	$\theta_{cm}$	$\frac{d\sigma}{dt}$	Rate	Yield	$E_\gamma$	$s$	$\theta_{cm}$	$\frac{d\sigma}{dt}$	Rate	Yield	$E_\gamma$	$s$	$\theta_{cm}$	$\alpha_n$	$\frac{d\sigma}{dt}$	Rate	Yield	
	GeV		Hrs	[GeV]	[GeV <sup>2</sup> ]	[deg]	$[\frac{pb}{GeV^2}]$	$[\frac{cnt}{Hr}]$	# evts	[GeV]	[GeV <sup>2</sup> ]	[deg]	$[\frac{pb}{GeV^2}]$	$[\frac{cnt}{Hr}]$	# evts	[GeV]	[GeV <sup>2</sup> ]	[deg]		$[\frac{pb}{GeV^2}]$	$[\frac{cnt}{Hr}]$	# evts	
1	2.2	<sup>3</sup> He	1	0.83	12.6	90	4000.0	38000	38000	2.20	11.8	142	720	760	760								
2	2.2	<sup>3</sup> He	6							2.20	11.8	90	1.15	1.9	17	100							
3	2.2	<sup>3</sup> He	4							2.20	11.8	90	0.90	2.8	26	110							
4	2.2	<sup>3</sup> He	2	1.65	17.1	90	21.0	200	390	2.20	11.8	90	340	360	710								
5	2.2	<sup>3</sup> He	2							2.20	11.8	90	1.10	5.7	54	110							
6	2.2	<sup>3</sup> He	1							2.20	11.8	30	1.0	99	950	950							
7	2.2	<sup>3</sup> He	1							2.20	11.8	37	1.0	58	560	560							
8	2.2	<sup>3</sup> He	5	1.85	18.3	90	6.7	65	320	2.20	11.8	70	590	620	3100								
9	2.2	<sup>3</sup> He	2							2.20	11.8	90	1.0	17	160	320							
10	2.2	<sup>3</sup> He	1							2.20	11.8	53	1.0	35	330	330							
11	2.2	<sup>3</sup> He	9	1.98	19.0	90	3.5	34	310	2.20	11.8	53	800	840	7600								
12	2.2	<sup>3</sup> He	2							2.20	11.8	70	1.0	25	240	490							
13	2.2	<sup>3</sup> He	16	2.09	19.6	90	2.1	20	320	2.20	11.8	30	3200	3300	53000								
14	2.2	<sup>3</sup> He	16							2.20	11.8	90	0.85	0.7	6	100							
15	2.2	d	1	$\gamma$ d $\rightarrow$ pn calibration run												2.20	11.8	90	1.0	1150	8400	8400	
16	4.4	d	24	$\gamma$ d $\rightarrow$ pn calibration run												4.40	20.0	90	1.0	2.76	21	500	
17	4.4	<sup>3</sup> He	222							4.40	20.0	90	1.0	0.02	0.45	100							

the  ${}^3\text{He}(\gamma,\text{pn})\text{p}$  reaction, rates were estimated using the  $\text{d}(\gamma,\text{pn})$  cross section [18], taking into account the calculated detection acceptance and the neutron detection efficiency. The neutron detection efficiency for each layer of HAND is about 2%. For 6 layers, taking into account a 50% attenuation by the lead wall, we get a total neutron detection efficiency of  $D_{eff} = 6\%$ . See appendix A for details about HAND efficiency calculation.

We will also form single arm measurements of  $\gamma d \rightarrow p+n$  to enable direct comparison of the cross sections of a free p-n pair and a p-n pair within  ${}^3\text{He}$  at the same kinematics. The yields in Table 1 for the deuteron target were projected from previous results.

## 2.9 Systematic uncertainties

The systematic uncertainties involved in the cross section calculation were thoroughly studied in the analysis of E03-101. They are governed by:

- The number of Bremsstrahlung photons per electron taken from theory [38].
- The evaluation of the two coincident protons acceptance of the two HRS, which is done by simulation. The simulation depends on the wave function of the spectator neutron taken from theory.

The total systematic uncertainty in the scaled cross section is estimated to be less than 7% for the proposed kinematics.

## 2.10 Random coincidence rate calculation

For  ${}^3\text{He}(\gamma,\text{pp})\text{n}$  and  ${}^3\text{He}(\gamma,\text{pd})$ , data from E03-101 shows that the contamination of the data by random proton and deuteron accidentals is negligible. For the  ${}^3\text{He}(\gamma,\text{pn})\text{p}$  channel, the random coincidence rate is calculated in appendix A. The optimized detection threshold was found to be 20-50 MeVee, which will result in a  $\sim 10\%$  statistical uncertainty at most for all  ${}^3\text{He}(\gamma,\text{pn})\text{p}$  data points.

# 3 Kinematics and requested beam time

## 3.1 ${}^3\text{He}(\gamma,\text{pp})\text{n}$

We propose to measure the  $\theta_{\text{c.m.}} = 90^\circ$  cross section at  $E_\gamma = 2.2$  and 4.4 GeV and the  $\alpha_n$  distribution at 2.2 GeV.

## 3.2 Simultaneous measurement of ${}^3\text{He}(\gamma,\text{pd})$ and ${}^3\text{He}(\gamma,\text{pn})\text{p}$

We also propose to measure simultaneously the  $\theta_{\text{c.m.}} = 90^\circ$   $\gamma^3\text{He} \rightarrow \text{pd}$  cross section and the angular distribution of  $\gamma^3\text{He} \rightarrow \text{pn}$  using an electron beam of  $E_e = 2.2$  GeV. The proposed kinematic settings (see Table 2) correspond to photon energies in the range of 0.83 GeV to 2.1 GeV in the  $\gamma^3\text{He} \rightarrow \text{pd}$  system, and to c.m. angles in the range of 30 to 142 degrees for the  $\gamma^3\text{He} \rightarrow \text{pn}$  system. The proposed data points and expected statistical uncertainties are plotted in Figures 2 and 5. The kinematic settings were selected to match the available  $\text{d}(\gamma,\text{p})\text{n}$  data. The cross sections and count rates have been calculated based on interpolation from JLab E03-101 and E99-008 data, assuming 50  $\mu\text{A}$  current, a 6 % copper radiator and the Hall A unpolarized  ${}^3\text{He}$  target.

The beam time request is summarized in Table 3 for a total of 19 days.

Table 2: *Kinematic settings.*

	$\theta_{HRS-L}$	$P_{HRS-L}$	$\theta_{HRS-R}$	$P_{HRS-R}$	$\theta_n$	$P_n$
	[deg]	$[\frac{GeV}{c}]$	[deg]	$[\frac{GeV}{c}]$	[deg]	$[\frac{GeV}{c}]$
1	105.43	0.917	39.34	1.394	19.88	2.599
2	49.71	1.803	49.71	1.803		
3	54.42	1.805	54.42	1.805		
4	52.54	1.808	69.13	1.536	52.53	1.808
5	50.66	1.806	50.66	1.806		
6	15.56	2.674	117.68	0.810		
7	19.34	2.609	106.84	0.902		
8	38.71	2.157	82.77	1.359	69.02	1.444
9	52.54	1.808	52.53	1.808		
10	28.33	2.415	86.30	1.149		
11	28.33	2.415	97.27	1.156	86.30	1.149
12	38.71	2.157	69.02	1.444		
13	15.56	2.674	124.30	0.869	117.68	0.810
14	55.38	1.801	55.38	1.801		
15	52.54	1.808	52.53	1.808		
16	42.72	2.990	42.72	2.990		
17	42.72	2.990	42.72	2.990		

Table 3: *Summary of the requested beam time.*

Measurement	Time
	[days]
Setup & Checkout	1
Measurement at 2.2 GeV on $^3\text{He}$ target 15 Kinematic changes 5 movements of HAND, scheduled one per day	6
Measurement at 2.2 GeV, 4.4 GeV on d target 2 target changes 1 energy change	2
Measurement at 4.4 GeV	10
<b>TOTAL REQUESTED BEAM TIME</b>	<b>19</b>

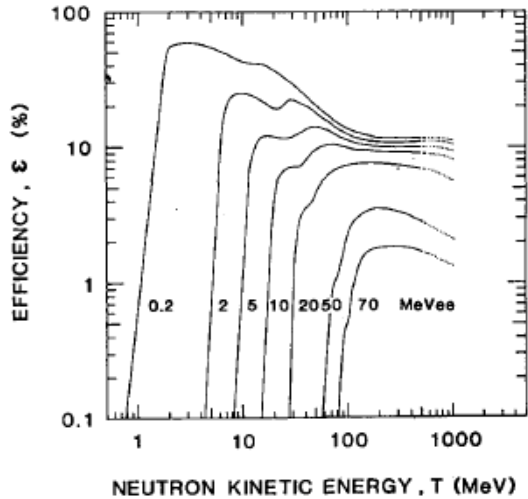


Figure 10: Neutron detection efficiencies calculated with the code of Cecil et al. [39]. Detector pulse-height thresholds are given in MeV equivalent electron energy (MeV ee). Plot is taken from [40].

## 4 Summary

In this document we propose to take high energy data for the  ${}^3\text{He}(\gamma,pp)n$ ,  ${}^3\text{He}(\gamma,pn)p$ , and  ${}^3\text{He}(\gamma,pd)$  reactions in high momentum-transfer kinematics. The high statistics cross section measurements will attempt to validate CCR to the highest degree of scaling ever observed and to determine whether deviation from CCR exists in the form re-scattering. The proposed measurement will be done in Hall A, uses standard Hall A equipment and requires very short setup time. The beam time request is for 19 days. High statistics data for  ${}^3\text{He}(\gamma,pp)n$  and  ${}^3\text{He}(\gamma,pd)$  is available from previous Hall A measurements.

The above conditions make this proposal an ideal 12 GeV commissioning experiment for Hall A.

## Appendix A: ${}^3\text{He}(\gamma,pn)p$ Random coincidence rate calculation

The uncertainty involved with subtracting random coincidence events can be minimized by placing an optimal detection threshold on HAND. Fig. 10 (taken from [40]) shows the detection efficiency for a 10 cm plastic scintillator for different threshold values in the range of 0.2 – 70 MeV equivalent electron (MeVee), calculated with the code of Cecil et al. [39]. HAND consists of 6 scintillator planes, each with 10 cm width, which yields an overall efficiency of:

$$\epsilon_{HAND} = 0.5 \cdot (1 - (1 - \epsilon_n)^6), \quad (4)$$

where 0.5 is the expected attenuation of the lead wall and  $\epsilon_n$  is the single scintillator plane efficiency taken from Fig. 10.

In order to evaluate p-n accidental detection rates, we first evaluate proton and neutron singles rates for the proposed luminosity. The proton singles rate is taken from E03-101 data at  $E_{beam}=2.1$  GeV (scaled to a current of 50  $\mu\text{A}$ ):

$$Rate_p(\text{proposed}) = 1.4[\text{kHz}] \quad (5)$$

To evaluate the neutron singles rate, we use a calculation by Degtyarenko [41, 42] of e

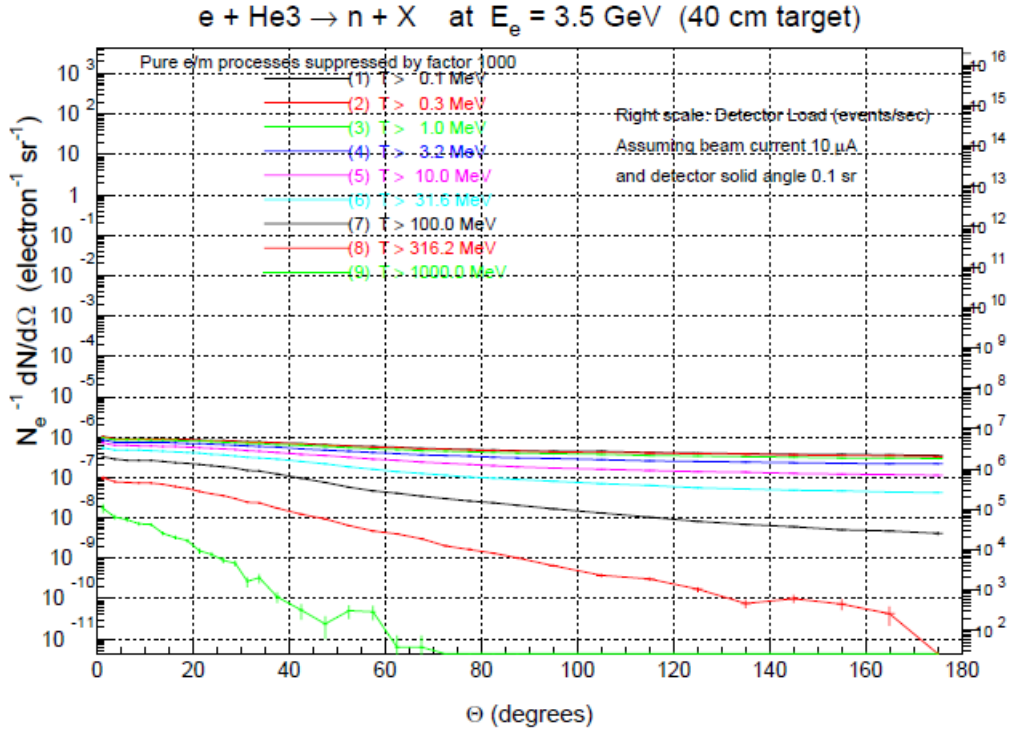


Figure 11: The neutron singles yield with kinetic energy above a given thresholds. Calculated in [41, 42].

+  $^3\text{He} \rightarrow n + X$  rates, as shown in Fig. 11. For  $55^\circ$ , we calculate the neutron singles rates ( $Rate_n(Degtyarenko)$ ) as a function of the minimal kinetic energy of the detected neutron. The later is determined from Fig. 10 as a function of the threshold. The values in Fig. 11 are given for a solid angle of 100 msr, and nucleon luminosity of

$$L(Degtyarenko) = 5 \cdot 10^{36} [\text{sec}^{-1} \text{cm}^{-2}]. \quad (6)$$

Table 4 summarizes the nucleon luminosity of the  $^3\text{He}$  cryotarget we plan to use. The total luminosity of the target is therefore:

$$L(proposed) = 3.3 \cdot 10^{38} [\text{sec}^{-1} \text{cm}^{-2}] \quad (7)$$

The solid angle of the HAND detector is:

$$\Delta\Omega_n(proposed) = \frac{A_{HAND}}{A_{4\pi}} = \frac{1[m] \cdot 3[m]}{(17[m])^2} = 10[m\text{sr}] \quad (8)$$

Using this information we can now scale the rates of [41, 42] to obtain an estimate for the singles rate of the proposed setup:

$$Rate_n(proposed) = Rate_n(Degtyarenko) \cdot \epsilon_{HAND} \cdot \frac{L(proposed)}{L(Degtyarenko)} \cdot \frac{\Delta\Omega_n(proposed)}{\Delta\Omega(Degtyarenko)} \quad (9)$$

The n-p random coincidence rate can now be estimated as:

$$Rate_{Random} = Rate_p \cdot Rate_n \cdot t_{resolv} \quad (10)$$

Table 5 shows the random coincidence uncertainty calculation for different values of pulse-height detection threshold. The values are calculated for the  $90^\circ$  c.m. data point

	Thickness (cm)	Density (gr/cm <sup>3</sup> )	Luminosity for I=50 $\mu$ A (sec <sup>-1</sup> cm <sup>-2</sup> )
Entrance window (Al)	0.0347	2.81	$1.8 \cdot 10^{37}$
Exit window (Al)	0.0300	2.81	$1.6 \cdot 10^{37}$
<sup>3</sup> He	20	0.079	$3.0 \cdot 10^{38}$
Total			$3.3 \cdot 10^{38}$

Table 4: Cryotarget nucleon luminosity for 50  $\mu$ A beam.

Thresh- hold	Minimal neutron kinetic energy	Plane eff ( $\epsilon_n$ )	HAND eff ( $\epsilon_{HAND}$ )	Proton- neutron Coinc. rate	Proton singles rate	Neutron singles rate	Rndm. coinc. rate	Signal events (S)	Rndm. events (N)	$\frac{\sqrt{S+2N}}{S}$
MeVee	MeV	%	%	Hz	kHz	kHz	Hz	Cnts	Cnts	%
0.2	1	12	27	0.46	1.4	6400	18	3300	130000	15
2	6	10	23	0.4	1.4	4800	13	2900	97000	15
5	12	9	22	0.37	1.4	3700	10	2600	75000	15
10	20	8	20	0.34	1.4	2700	7.6	2400	54000	14
20	40	5.5	14	0.25	1.4	1500	4.1	1800	30000	14
50	80	2	5.7	0.097	1.4	78	0.22	700	1600	8.9
70	120	1.2	3.5	0.06	1.4	72	0.2	430	1400	13

Table 5: The rates and statistical uncertainty for the <sup>3</sup>He( $\gamma$ ,pn)p measurement. The calculation is given for different values of detection threshold. The threshold value of choice is highlighted.

which has the lowest projected rate of all the proposed  $\gamma$   $^3\text{He} \rightarrow \text{pn}$  data points, under the assumption of 2 hours of beam time. The resolving time is taken to be 2 ns.

For a threshold value of 50 MeVee, with the expected signal rate and available beam time (determined by other considerations) we expect to measure the  $^3\text{He}(\gamma, \text{pn})\text{p}$  cross section with statistical uncertainty better than 10% at all proposed kinematics.

Comment: For the detection of 1-2 GeV/c neutrons a better neutron detection is possible by introducing absorbers between the scintillators, as was done in BigHand for the GEN measurement [43]. In our case the limiting factor is the necessity to move the detector to a few positions. The calculation given here shows that for the projected rates, beam time, and neutron energies of the proposed measurement, the current HAND detector is sufficient.

## References

- [1] Stanley J. Brodsky and Glennys R. Farrar. Scaling Laws at Large Transverse Momentum. *Phys. Rev. Lett.*, 31:1153–1156, 1973.
- [2] V. A. Matveev, R. M. Muradian, and A. N. Tavkhelidze. Automodellism in the large - angle elastic scattering and structure of hadrons. *Nuovo Cim. Lett.*, 7:719–723, 1973.
- [3] G. Peter Lepage and Stanley J. Brodsky. Exclusive Processes in Perturbative Quantum Chromodynamics. *Phys. Rev.*, D22:2157, 1980.
- [4] Xiangdong Ji, Jian-Ping Ma, and Feng Yuan. Generalized counting rule for hard exclusive processes. *Phys. Rev. Lett.*, 90(24):241601, Jun 2003.
- [5] Joseph Polchinski and Matthew J. Strassler. Hard scattering and gauge / string duality. *Phys. Rev. Lett.*, 88:031601, 2002.
- [6] A. Danagoulian et al. Compton-scattering cross section on the proton at high momentum transfer. *Phys. Rev. Lett.*, 98(15):152001, Apr 2007.
- [7] M. Sargsian. private communication.
- [8] Gerald A. Miller. Handling the handbag diagram in compton scattering on the proton. *Phys. Rev. C*, 69(5):052201, May 2004.
- [9] Archibald W. Hendry. Evidence for coherent effects in large-angle hadron-hadron scattering. *Phys. Rev. D*, 10(7):2300–2303, Oct 1974.
- [10] Stanley J. Brodsky and Guy F. de Teramond. Spin correlations, qcd color transparency, and heavy-quark thresholds in proton-proton scattering. *Phys. Rev. Lett.*, 60(19):1924–1927, May 1988.
- [11] Bernard Pire and John P. Ralston. Fixed angle elastic scattering and the chromocoulomb phase shift. *Physics Letters B*, 117(3-4):233 – 237, 1982.
- [12] P. V. Landshoff. Model for elastic scattering at wide angle. *Phys. Rev. D*, 10(3):1024–1030, Aug 1974.
- [13] J. Napolitano et al. Measurement of the differential cross-section for the reaction H-2 ( $\gamma$ , p) n at high photon energies and theta (c.m.) = 90-degrees. *Phys. Rev. Lett.*, 61:2530–2533, 1988.

- [14] S. J. Freedman et al. Two-body disintegration of the deuteron with 0.8-GeV to 1.8-GeV photons. *Phys. Rev.*, C48:1864–1878, 1993.
- [15] J. E. Belz et al. Two body photodisintegration of the deuteron up to 2.8- GeV. *Phys. Rev. Lett.*, 74:646–649, 1995.
- [16] C. Bochna et al. Measurements of deuteron photodisintegration up to 4.0- GeV. *Phys. Rev. Lett.*, 81:4576–4579, 1998.
- [17] E. C. Schulte et al. Measurement of the high energy two-body deuteron photodisintegration differential cross-section. *Phys. Rev. Lett.*, 87:102302, 2001.
- [18] E. C. Schulte et al. High energy angular distribution measurements of the exclusive deuteron photodisintegration reaction. *Phys. Rev.*, C66:042201, 2002.
- [19] M. Mirazita et al. Complete angular distribution measurements of two-body deuteron photodisintegration between 0.5-GeV and 3-GeV. *Phys. Rev.*, C70:014005, 2004.
- [20] P. Rossi et al. Onset of asymptotic scaling in deuteron photodisintegration. *Phys. Rev. Lett.*, 94:012301, 2005.
- [21] I. Pomerantz et al. Hard photodisintegration of a proton pair. *Physics Letters B*, 684(2-3):106 – 109, 2010.
- [22] S. J. Brodsky et al. Hard photodisintegration of a proton pair in He-3. *Phys. Lett.*, B578:69–77, 2004.
- [23] Misak M. Sargsian and Carlos Granados. Hard Break-Up of Two-Nucleons from the  $^3\text{He}$  Nucleus. *Phys. Rev.*, C80:014612, 2009.
- [24] Stanley J. Brodsky and John R. Hiller. Reduced nuclear amplitudes in quantum chromodynamics. *Phys. Rev.*, C28:475, 1983.
- [25] V. Yu. Grishina et al. Deuteron photodisintegration within the quark gluon strings model and QCD motivated nonlinear Regge trajectories. *Eur. Phys. J.*, A10:355–364, 2001.
- [26] V. Yu. Grishina et al. Polarization observables in high-energy deuteron photodisintegration within the quark gluon strings model. *Eur. Phys. J.*, A18:207–209, 2003.
- [27] Leonid L. Frankfurt, Gerald A. Miller, Misak M. Sargsian, and Mark I. Strikman. QCD rescattering and high energy two-body photodisintegration of the deuteron. *Phys. Rev. Lett.*, 84:3045–3048, 2000.
- [28] J. Alcorn et al. Basic Instrumentation for Hall A at Jefferson Lab. *Nucl. Instrum. Meth.*, A522:294–346, 2004.
- [29] B. A. Mecking et al. The CEBAF Large Acceptance Spectrometer (CLAS). *Nucl. Instrum. Meth.*, A503:513–553, 2003.
- [30] V. Isbert et al. Two-body photodisintegration of He-3 between 200-MeV and 800-MeV. *Nucl. Phys.*, A578:525–541, 1994.
- [31] I. Pomerantz, Y.Ilieva, et al. to be submitted for publication, *Phys. Rev. Lett.*
- [32] Misak M. Sargsian. Selected topics in high energy semi-exclusive electro- nuclear reactions. *Int. J. Mod. Phys.*, E10:405–458, 2001.

- [33] R. Schiavilla. Induced Polarization in the  ${}^2\text{H}(\gamma, \vec{n}){}^1\text{H}$  Reaction at Low Energy. *Phys. Rev.*, C72:034001, 2005.
- [34] S. Gilad et al. JLab proposal PR05-102: Measurements of Ax and Az Asymmetries in the Quasi-elastic  ${}^3\text{He}(e, e'd)$  Reaction.
- [35] T. Averett et al. Jlab proposal pr08-005: Measurement of the target single-spin asymmetry, ay, in the quasi-elastic  ${}^3\text{he}(e, e'n)$  reaction.
- [36] S. Gilad et al. Jlab proposal pr07-006: Studying short-range correlations in nuclei at the repulsive core limit via the triple coincidence  $(e, e'pn)$  reaction.
- [37] P. E. Ulmer. Mceep: Monte carlo for electro-nuclear coincidence experiments. 1991. CEBAF-TN-91-101.
- [38] L. Tiator and L. E. Wright. VIRTUAL PHOTONS IN PION ELECTROPRODUCTION. *Nucl. Phys.*, A379:407–414, 1982.
- [39] R. A. Cecil, B. D. Anderson, and R. Madey. Improved predictions of neutron detection efficiency for hydrocarbon scintillators from 1 mev to about 300 mev. *Nuclear Instruments and Methods*, 161(3):439–447, 1979.
- [40] R. Madey, J.W. Watson, M. Ahmad, B.D. Anderson, A.R. Baldwin, A.L. Casson, W. Casson, R.A. Cecil, A. Fazely, J.M. Knudson, C. Lebo, W. Pairsuwan, P.J. Pella, J.C. Varga, and T.R. Witten. Large volume neutron detectors with subnanosecond time dispersions. *Nuclear Instruments and Methods in Physics Research*, 214(2-3):401 – 413, 1983.
- [41] P. Degtyarenko. Applications of the photonuclear fragmentation model to radiation protection problems. CEBAF-PR-95-66.
- [42] P. Degtyarenko, M. Kossov, and H. Wellisch. Chiral invariant phase space event generator. *The European Physical Journal A - Hadrons and Nuclei*, 8:217–222, 2000. 10.1007/s100500070108.
- [43] B. Wojtsekhowski et al. JLab proposal PR02-013: Measurement of the Neutron Electric Form Factor GEn at High Q<sup>2</sup>.